635

DATASET · MARCH 2014

READS
157

5 AUTHORS, INCLUDING:

Adriana Szeghalmi
Friedrich Schiller University Jena
51 PUBLICATIONS **731** CITATIONS
SEE PROFILE

Michael Schmitt
Northwestern University
1,639 PUBLICATIONS **19,497** CITATIONS
SEE PROFILE

Juergen Popp
Friedrich Schiller University Jena
407 PUBLICATIONS **6,061** CITATIONS
SEE PROFILE

Wolfgang Kiefer
University of Wuerzburg
878 PUBLICATIONS **9,847** CITATIONS
SEE PROFILE

JOURNAL OF RAMAN SPECTROSCOPY
J. Raman Spectrosc. 2003; **34**: 413–419
Published online in Wiley InterScience (www.interscience.wiley.com). DOI: 10.1002/jrs.1013

JRS

Density functional and vibrational spectroscopic analysis of β-carotene

S. Schlücker, A. Szeghalmi, M. Schmitt, J. Popp† and W. Kiefer*

Institut für Physikalische Chemie der Universität Würzburg, Am Hubland, D-97074 Würzburg, Germany

Received 2 December 2002; Accepted 28 March 2003

We report a computational study on the structural, energetic and vibrational spectroscopic characteristics of β-carotene employing density functional theory (DFT). The optimized geometry and the complete vibrational spectrum calculated at the BPW91/6–31G* level, including infrared (IR) intensities and Raman activities, are presented. The centrosymmetric structure of β-carotene is verified both theoretically and experimentally, by identifying a stable calculated structure with C_i symmetry and the mutually exclusive occurrence of bands in the experimental Fourier transform IR and Raman spectrum, respectively. The calculated vibrational spectra reflect the major characteristic features observed experimentally. Differences in the calculated IR intensities and Raman activities for a few dominant modes of two β-carotene configuration isomers, the all-*trans* and the natural abundant (C_6–C_7) s-*cis* form, are explained qualitatively by the corresponding eigenvectors. At the level of theory employed, s-*cis*-β-carotene was found to be 8.8 kJ mol^{-1} more stable than the all-*trans* form. Calculations on β-carotene model systems were performed to separate electronic from steric contributions. The higher stability of s-*cis*-β-carotene is explained by an energetically favored β-ionone ring conformation, compensating for its shorter conjugation length in comparison with the all-*trans* form. Copyright © 2003 John Wiley & Sons, Ltd.

KEYWORDS: density functional theory; β-carotene; configurational isomers

INTRODUCTION

Terpenoids, also termed terpenes or isoprenoids, belong to a diverse and widespread class of natural products, which are the formal polymerization products of isoprene. According to the number of isoprene units, terpenoids are classified as mono- (C_{10}), sesqui- (C_{15}), di- (C_{20}), sester- (C_{25}) triterpenoids (C_{30}), carotenoids (C_{40}) and polyisoprenoids.[1] Among the carotenoids are carotenes and xanthophylls, which are hydrocarbons and oxygen-containing derivatives, respectively. Carotenoids show yellow to red colors because of their large number of conjugated double bonds. In particular, β-carotene consists of a polyene chain with nine conjugated double bonds and two β-ionone rings. It is the biosynthetic precursor of vitamin A_1 or retinol, which is formed by the cleavage of β-carotene at the central double bond. By oxidation of this primary alcohol to an aldehyde, rhodopsin is formed. Rhodopsin undergoes a series of photochemical reactions after irradiation with visible light, yielding activated rhodopsin or all-*trans*-retinalopsin. Finally, an electrical signal in the rod cells of vertebrates is generated.[2] In addition to its importance in the process of vision, a second important biological function of β-carotene is to serve as an accessory pigment in photosynthesis. All photosynthetic organisms such as plants and diverse bacteria contain chlorophyll a. Molecules such as chlorophyll b, xanthophylls and carotenoids including β-carotene are present in accessory pigments which absorb light that chlorophyll a does not absorb.[2]

Carotenoids and β-carotene in particular have been extensively studied by various spectroscopic methods. Among them are vibrational spectroscopic techniques such as resonance Raman (RR) spectroscopy[3–11] and Raman spectroscopy with near-infrared (NIR) excitation.[11–13] The first normal coordinate analysis (NCA) of a β-carotene model system was published 20 years ago by Saito and Tasumi.[3] In a more recent work on β-carotene and several xanthophylls, semi-empirical calculations (AM1 level) were reported and special emphasis was put on understanding the electronic absorption spectra and on the comparison of

*Correspondence to: W. Kiefer, Institut für Physikalische Chemie der Universität Würzburg, Am Hubland, D-97074 Würzburg, Germany. E-mail: wolfgang.kiefer@mail.uni-wuerzburg.de
†Present address: Institut für Physikalische Chemie, Friedrich-Schiller-Universität Jena, Helmholtzweg 4, D-07743 Jena, Germany.
Contract/grant sponsor: Deutsche Forschungsgemeinschaft;
Contract/grant number: GRK 690/1.
Contract/grant sponsor: Fonds der Chemischen Industrie.

Raman spectra obtained under resonant versus non-resonant conditions.[11] In order to calculate molecular properties accurately, however, inclusion of electron correlation is required. In addition to post-Hartree–Fock (HF) methods such as Møller–Plesset (MP) perturbation theory, DFT has become very popular because of its good performance at reasonable computational costs.[14] The influence of electron correlation on energies and geometries of retinal and its derivatives, for example, was calculated with DFT.[15] In other studies, the photoisomerization pathway of a retinal chromophore model was examined. Because of their scaling with the number of electrons and basis functions entering the configurational state functions (CSF),[16] these high-level *ab initio* methods are computationally very expensive. Examples include the complete active space self-consistent field (CASSCF) method[17,18] and multi-configuration second-order perturbation theory (MCPT2).[19] In computational studies employing DFT in particular, the *trans–cis* isomerization in long linear polyene chains serving as β-carotene model systems[20] and the reaction of singlet oxygen with a carotenoid model system were, for example, investigated.[21] Although quantum chemical calculations on large molecular systems have become feasible nowadays, to the best of our knowledge, no *ab initio* or DFT calculations examining the structural, energetic and vibrational spectroscopic characteristics of β-carotene have been published so far.

The knowledge of structural and vibrational spectroscopic properties of β-carotene is highly desirable for different purposes. First, interactions such as hydrogen bonding between carotenoid and porphyrin moieties in light-harvesting complexes, for example, can be examined by computational chemistry.[22] Second, vibrational spectroscopic properties are required for both wavenumber- and time-resolved vibrational spectroscopic experiments. In wavenumber-resolved IR and Raman spectroscopy, an unambiguous assignment of vibrational bands to the corresponding normal modes is required. In time-resolved vibrational spectroscopy, probing photophysical processes such as the $S_1 \rightarrow S_0$ internal conversion in β-carotene, a visualisation of nuclear motions during normal modes is illustrative for understanding the phenomenon of vibronic coupling in polyatomic molecules.[23]

EXPERIMENTAL AND COMPUTATIONAL DETAILS

Measurements on β-carotene were carried out with a Fourier transform (FT) spectrometer (Bruker, Model IFS120 HR) equipped with a Raman module (Model FRA106). For IR spectroscopy on β-carotene prepared as a KBr pellet, a globar lamp and a mercury cadmium telluride (MCT) detector were employed. Raman excitation was provided with a Nd:YAG laser (1064 nm) and an InGaAs detector was used. Raman spectra of polycrystalline β-carotene were recorded in a backscattering geometry (180°) with a laser output power of ~300 mW. When employing NIR excitation at this power level, local heating cannot be excluded; no sample decomposition, however, was observed during the Raman measurements.

DFT calculations were carried out using the Gaussian 98 suite of programs[24] employing the pure density functional BPW91 and the 6–31G(d) or 6–31G* basis set. For β-carotene isomers and electronic model systems (see below), C_i symmetry constraints were used. Redundant internal coordinates were generated using the program MOLDEN.[25] IR intensities and Raman activities were calculated analytically.

RESULTS AND DISCUSSION

Optimized geometries

In Fig. 1, the constitution formulas of the two investigated isomers of β-carotene together with the labeling of the carbon skeleton are shown. Both configurational isomers are centrosymmetric molecules as indicated. The corresponding optimized geometries of (C_6–C_7) s-*cis*- and all-*trans*-β-carotene are displayed in Fig. 2(a) and (b). The calculation of vibrational spectra yielded only real (positive) wavenumber values, indicating that stable structures were identified. From Fig. 2(c) and (d), in which the carbon skeleton is presented in a side view, the local symmetry of the polyene chains and the conformation of the β-ionone rings are recognizable. The polyene chain is essentially planar, hence for this part of the molecule local C_{2h} symmetry can be assumed; for the β-ionone rings a twist conformation is observed. In the case of the s-*cis* isomer, shown in Fig. 2(a) and (c), the calculated dihedral angle C_5—C_6—C_7—C_8 of 42.9° indicates that the β-ionone rings are tilted by almost 45° relative to the molecular plane and that the terminal double bonds are only in partial conjugation with the polyene chain. In contrast, the calculated dihedral angle of 171.9° indicates almost complete conjugation with the polyene chain for the all-*trans* isomer. A comparison of the absolute energies of both isomers reveals that, despite of its reduced conjugation length, the s-*cis* isomer is 8.8 kJ mol^{-1} more stable than the all-*trans* form. Because the computational

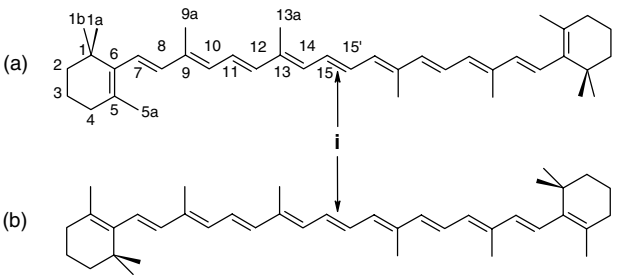

Figure 1. Constitution formulas of (C_6–C_7) s-*cis*- (a) and all-*trans*-β-carotene (b), together with the labeling of the carbon skeleton (center of inversion i).

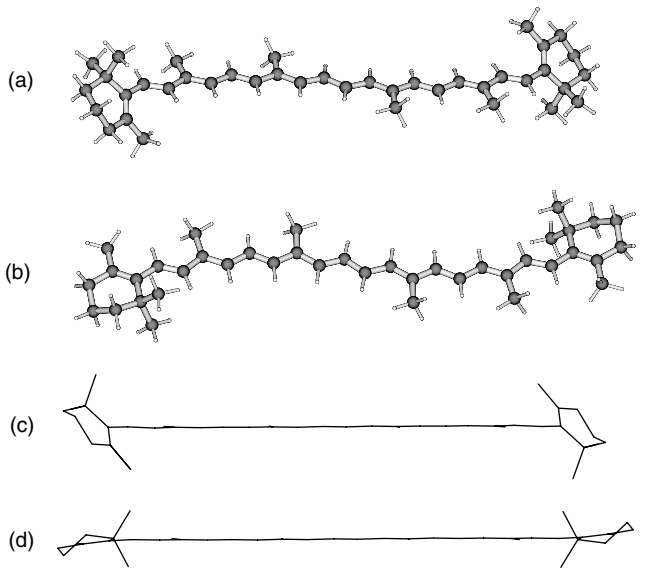

Figure 2. Geometries of s-*cis*- (a) and all-*trans*-β-carotene (b) optimized at the BPW91/6–31G* level. The carbon skeleton is shown in a different perspective in (c) and (d).

results refer to the gas phase, crystal packing effects can be excluded. A detailed analysis of this energetic aspect is given below. In the following, the characteristic structural parameters of β-carotene are discussed and a comparison of experimental and theoretical data is presented. In Table 1 selected experimentally observed[26] and calculated bond distances and angles of β-carotene are listed. Experimental values are taken from the x-ray structure of β-carotene with (C_6–C_7) s-*cis* configuration determined by Senge *et al*.[26] In general, alternating carbon–carbon bond lengths for the polyene chain are noted. The constitution formulas shown in Fig. 1 suggest alternating single and double bonds because of the used valence bond (VB) notation. For both experiment and theory, the expected delocalization of the π-electron system, as predicted by molecular orbital (MO) theory, is verified; the C—C bond distances of the polyene chain assume values between those found for single and double bonds. In comparison with the X-ray structure, the calculations overestimate the C—C single bond distances, e.g. C_1—$C_{1A/B}$, C_1—C_2 and C_6—C_7, by up to 0.022 Å or 2.2 pm at the level of theory employed. Similar deviations are observed for the C_{15}—$C_{15'}$ and the adjacent C_{14}—C_{15} bond. In general, the deviations of the theoretical values from the experimental data are considered to be small, with a mean deviation of 1.1% for the bond distances and 0.4% for the bond angles.

Table 1. Selected bond distances and bond angles of β-carotene: experimental data (C_6-C_7 s-*cis* configuration)[26] are compared with theoretical values, calculated at the BPW91/6–31G* level, for the s-*cis* and all-*trans* forms

	Exp. (s-*cis*)	Theo. (s-*cis*)	Theo. (s-*trans*)
Bond distance (Å)—			
C_1—C_{1A}	1.529	1.551	1.553
C_1—C_{1B}	1.528	1.552	1.554
C_1—C_2	1.529	1.551	1.555
C_1—C_6	1.531	1.553	1.551
C_2—C_3	1.526	1.529	1.528
C_3—C_4	1.526	1.531	1.529
C_4—C_5	1.523	1.517	1.514
C_5—C_{5A}	1.502	1.513	1.520
C_5—C_6	1.351	1.371	1.381
C_6—C_7	1.449	1.471	1.461
C_7—C_8	1.352	1.370	1.375
C_8—C_9	1.445	1.449	1.447
C_9—C_{9a}	1.500	1.512	1.512
C_9—C_{10}	1.352	1.386	1.388
C_{10}—C_{11}	1.442	1.429	1.427
C_{11}—C_{12}	1.352	1.382	1.383
C_{12}—C_{13}	1.444	1.437	1.435
C_{13}—C_{13a}	1.500	1.514	1.514
C_{13}—C_{14}	1.353	1.392	1.393
C_{14}—C_{15}	1.441	1.422	1.421
C_{15}—$C_{15'}$	1.346	1.386	1.387
Bond angle (°)—			
C_1—C_2—C_3	112.9	112.9	113.3
C_2—C_3—C_4	104.0	109.0	108.7
C_3—C_4—C_5	114.4	113.8	113.9
C_4—C_5—C_6	121.5	122.7	123.5
C_{5A}—C_5—C_6	125.9	124.4	123.7
C_1—C_6—C_5	122.1	122.1	121.2
C_5—C_6—C_7	122.2	122.8	117.6
C_6—C_7—C_8	126.7	126.4	131.1
C_7—C_8—C_9	127.2	126.3	125.4
C_8—C_9—C_{10}	119.1	118.2	118.0
C_{9a}—C_9—C_{10}	122.2	123.1	122.7
C_9—C_{10}—C_{11}	127.3	128.4	128.6
C_{10}—C_{11}—C_{12}	123.0	123.1	123.0
C_{11}—C_{12}—C_{13}	126.1	126.7	126.9
C_{12}—C_{13}—C_{14}	117.7	118.3	118.2
C_{13a}—C_{13}—C_{14}	122.9	122.8	122.8
C_{13}—C_{14}—C_{15}	127.7	128.3	128.6
C_{14}—C_{15}—$C_{15'}$	123.0	123.8	123.6

Vibrational spectra

Symmetry and computational considerations

The mutual exclusion principle in vibrational spectroscopy provides a simple but powerful criterion to test for the presence of a molecular center of inversion. The mutually exclusive occurrence of IR- and Raman-active modes in the experimental FT-IR and NIR-FT-Raman spectrum of β-carotene is indicated exemplarily for dominant bands by dotted lines in Fig. 3. To the best of our knowledge, this is the

JRS

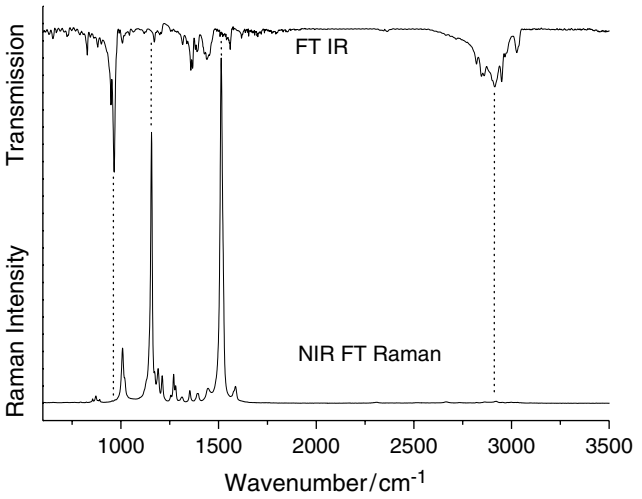

Figure 3. Experimental FT-IR and NIR-FT-Raman spectra of β-carotene.

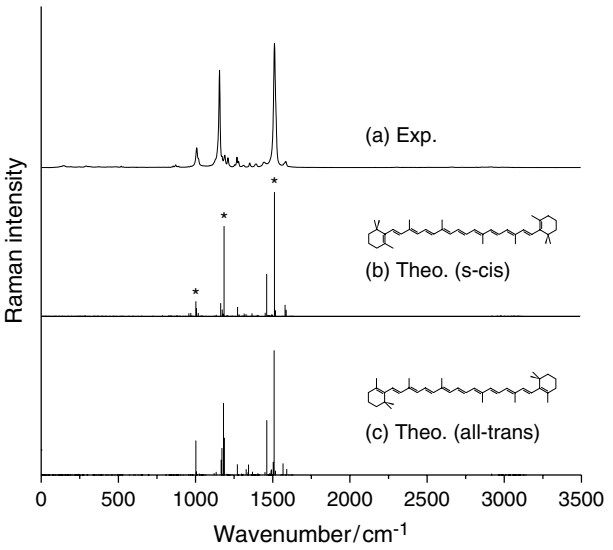

Figure 4. Experimental NIR-FT-Raman spectrum of β-carotene (a) and calculated Raman spectra of s-*cis*- (b) and all-*trans*-β-carotene (c).

first direct comparison of vibrational spectra of β-carotene giving evidence for its centrosymmetry. According to the employed symmetry constraints, all 282 normal modes of β-carotene were classified as either Raman active (a_g symmetry) or IR active (a_u symmetry). The aim of this paper is not to reproduce the experimental spectra to a high wavenumber precision, but to reflect the observed major general features and trends. In general, calculated harmonic wavenumber values differ to a certain extent from experimental data because of anharmonicity effects. Only in the case of very small molecules such as water, for which the anharmonicity constants the experimentally observed wavenumbers may be extrapolated to hypothetical harmonic values. The latter may then be compared with calculated harmonic values. A different approach includes the usage of scaling factors[27], a somehow empirical method even if transferable scaling factors[28] are used. Therefore, it must be clearly noted that the good agreement of the calculated harmonic wavenumbers with the experimentally observed values obtained in this study is attributed to the well-known error cancelation in DFT.

Comparison of experimental and calculated Raman spectra

In Fig. 4, the normalized experimental FT-Raman spectrum of β-carotene (a) and the normalized calculated Raman spectra of (C_6—C_7) s-*cis*- (b) and all-*trans*-β-carotene (c) are shown. The calculated spectra, (b) and (c), were corrected for the $\omega_0\omega_S^3$ intensity dependency of the Stokes photons (ω_S); ω_0 is the angular frequency corresponding to the 1064 nm line of the Nd:YAG laser employed. In general, considering the large number of 141 Raman-active modes, the experimental NIR-FT-Raman spectrum is dominated by few intense bands. The Raman intensities of the C–H stretching vibrations are extremely low, which is explained in terms of insufficient instrument/detector response in this spectral region. Because of the NIR excitation employed, the appearance of so-called overtones at $2\tilde{\nu}_i$ can presumably be excluded. The strongly differing Raman intensities of β-carotene normal modes can be understood in terms of their eigenvectors, which are presented for the first time in this paper. The calculated eigenvectors of the Raman bands indicated by an asterisk in Fig. 4 are shown in Fig. 5; for clarity of presentation, only eigenvectors at selected carbon atoms are shown. In Fig. 5(a), the eigenvectors of the CH_3 deformation mode, appearing at 1002 cm^{-1} in the calculated spectrum Fig. 4(b), are shown. The nuclear displacements along the polyene chain and the β-ionone rings explain the considerable Raman intensity observed experimentally. The largest changes in polarizability occur for the C—C and C═C stretching vibrations at 1185 and 1513 cm^{-1}, respectively; the corresponding eigenvector patterns are shown in Fig. 5(b) and 5(c). A comparison with Fig. 4(a) and 4(b) reveals that these modes give rise to the most intense bands in both the experimental and calculated Raman spectra. The eigenvectors of a β-ionone C–H stretching vibration at 2925 cm^{-1} are displayed in Fig. 5(d).

A significant deviation regarding the calculated and experimentally observed Raman intensity is noted for the band at 1463 cm^{-1} in Fig. 4(b). A possible explanation for this discrepancy is to regard it as the magnitude of possible errors in the calculated Raman activities of all normal modes. The approximate peak intensity ratio of the dominant modes at 1002, 1185 and 1513 cm^{-1} (0.13 : 0.73 : 1) observed in the calculated spectrum of the s-*cis* isomer in Fig. 4(b), however, reflects the observed experimental intensity ratio (0.15 : 0.79 : 1) in Fig. 4(a) fairly well. In contrast, the intensity ratio calculated for the all-*trans* isomer (0.28 : 0.58 : 1) differs significantly [Fig. 4(c)].

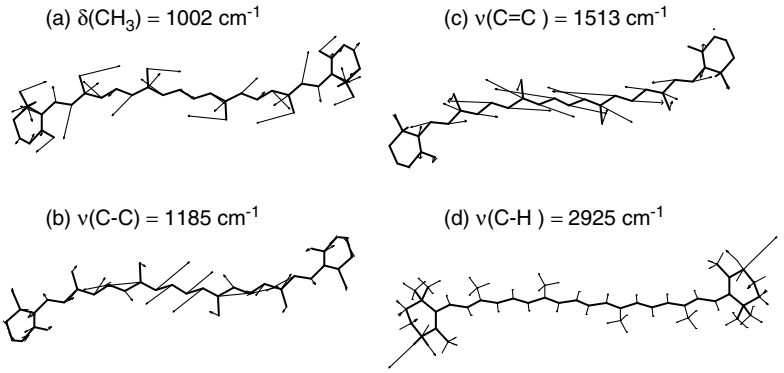

Figure 5. Normal-mode eigenvectors related to the bands indicated by an asterisk in Fig. 4: (a) CH_3 deformation; (b) C — C stretch; (c) C═C stretch; (d) C–H stretch.

Comparison of experimental and calculated IR Spectra

In Fig. 6, the normalized experimental FT-IR spectrum of β-carotene (a) and the normalized calculated IR spectra of s-*cis*- (b) and all-*trans*- β-carotene (c) are shown for the wavenumber range 600–3500 cm^{-1}. In the calculated IR spectra, the strongest absorption for the s-*cis* isomer is observed in the C–H stretching region at 3051 cm^{-1}; the IR spectrum of the all-*trans* form is dominated by the absorption band at 1550 cm^{-1}, which is assigned to the C═C stretching vibration of the polyene chain. The calculated IR intensities for this mode in both β-carotene configuration isomers differ significantly, which can be explained by the corresponding eigenvectors shown in Fig. 7. For clarity of presentation, only eigenvectors for selected atoms on the left side of the polyene chain are shown in Fig. 7(a) and 7(b). In the case of the C═C stretching vibration, the eigenvectors of the polyene chain and β-ionone ring atoms are nearly perpendicular for the s-*cis* isomer (a); in contrast, they are almost parallel for the all-*trans* form (b). The differences in the resulting transition dipole moment account for the larger calculated IR intensity of this mode in the all-*trans* form in comparison with the s-*cis* isomer. A similar explanation holds for the calculated IR intensities of the band at 3051 cm^{-1}; the corresponding eigenvectors are shown in Fig. 7(c) and 7(d), respectively. The dominant absorption band at 977 cm^{-1} in the experimental spectrum shown in Fig. 7(a) is assigned predominantly to an out-of-plane deformation mode of the polyene chain, with minor contributions from the β-ionone rings. This in-phase wagging vibration, involving hydrogen atoms (C═C—H) and methyl groups (C—C—Me), results into a large transition dipole moment perpendicular to the molecular plane; the calculated absorption for this mode in the s-*cis* isomer is ~4.5 times larger than in the all-*trans* form.

Energetic considerations

Subtle structural and energetic differences in biological molecules, such as ruffling in metalloporphyrins, have been revealed by DFT calculations.[29,30] In order to explain our

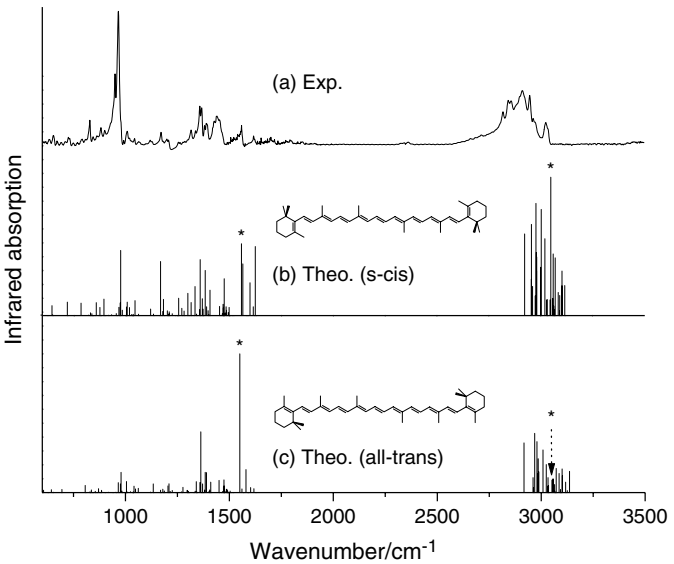

Figure 6. Experimental FT-IR spectrum of β-carotene (a) and calculated IR spectra of s-*cis*- (b) and all-*trans*-β-carotene (c).

JRS

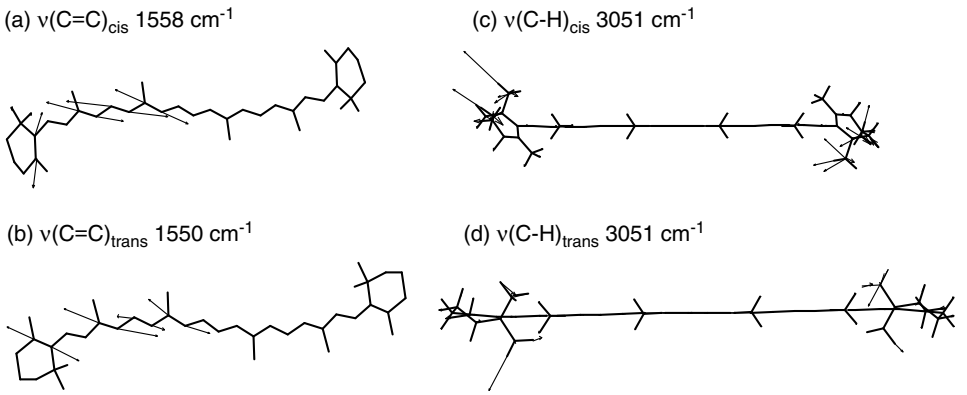

Figure 7. Normal-mode eigenvectors related to the bands indicated by an asterisk in Fig. 6: C═C (a, b) and C–H (c, d) stretching vibrations of s-*cis*- and all-*trans*-β-carotene, respectively.

finding mentioned above, that the natural abundant s-*cis* isomer of β-carotene is 8.8 kJ mol^{-1} more stable than the all-*trans* isomer, appropriate model systems were investigated. One basic assumption is that two contrary effects influence the absolute energy. On the one hand, effects such as conjugation of the polyene system stabilize the system; on the other hand, steric interactions, induced by the methyl substituents of the polyene chain and by the β-ionone rings, destabilize the molecule. A methyl-substituted undecene derivative [see Fig. 8(a) and (b)] was used as a model system to study conjugation effects. According to the methyl substitution at the terminal double bonds, the undecene model system has similar electronic properties compared with β-carotene. For this model system, energetic effects due to the conjugation length and steric effects induced by the methyl groups are separated from ring torsions. Figure 8 shows the optimized geometries of the s-*cis* (c) and all-*trans* (d) electronic model system. In contrast to β-carotene, the all-*trans* electronic model system is 27.2 kJ mol^{-1} more stable than the corresponding s-*cis* form. The terminal double bonds in the s-*cis* model system [Fig. 8(c)] are tilted by 39.3° relative to the polyene chain, which resembles the findings for s-*cis*-β-carotene. Because ring torsional effects can be excluded for the electronic model system, it is assumed that repulsive interactions between the methyl group and the polyene chain cause the observed deviation from planarity. In contrast, for the all-*trans* electronic model system [Fig. 8(d)], a dihedral angle C_5—C_6—C_7—C_8 of 179.7° was found, indicating that the terminal double bonds are in conjugation with the polyene chain. The observed minor deviation from planarity for all-*trans*-β-carotene, for which this dihedral angle is 171.9°, is attributed to the influence of the β-ionone rings on the overall molecular structure. Based on these findings, we assume that β-ionone ring torsions in s-*cis*-β-carotene are reduced in comparison with its all-*trans* form. In order to support this hypothesis, β-ionone model systems were investigated, in which the C_7 methyl group was substituted by hydrogen [Fig. 8(e)]. The C_6—H bond distance was taken as 1.09 Å, i.e. a value similar to the C—H bond distances of the polyene chain. The absolute energies were determined via single point calculations for the conformations in which the β-ionone rings are present in s-*cis*- and all-*trans*-β-carotene, respectively [see Fig. 2(a) and (b)]. For a single ring the energy difference at the level of theory employed is 10.0 kJ mol^{-1} in favor of the ring conformation present in s-*cis*-β-carotene. Thus, we have demonstrated that reduced ring torsion effects are responsible for the higher stability of natural abundant s-*cis*-β-carotene in comparison with its all-*trans* isomer.

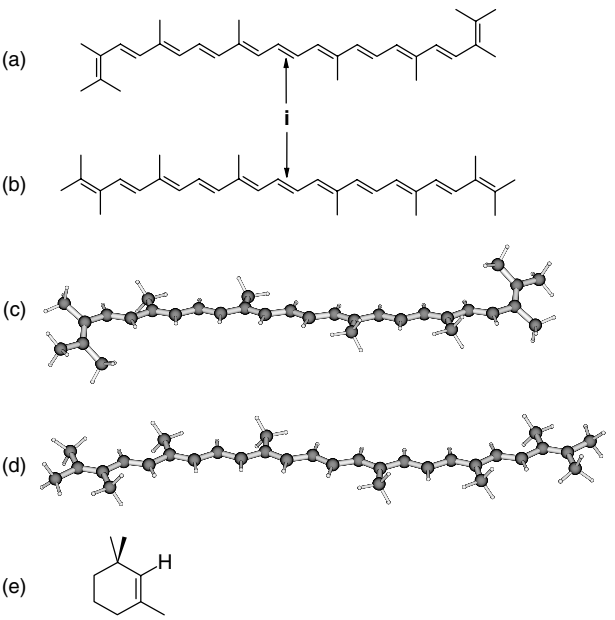

Figure 8. Formulas of β-carotene model systems used to study electronic effects: (a) s-*cis*- and (b) all-*trans*- undecene derivative. The corresponding geometries, optimized at the BPW91/6–31G* level, are shown in (c) and (d). In (e), the β-ionone ring system employed for conformational studies is displayed.

CONCLUSIONS

A computational study on β-carotene employing DFT is presented and the results are compared with vibrational spectroscopic data from FT-IR and NIR-FT-Raman experiments. The geometries and vibrational spectra of two configuration isomers of β-carotene were calculated at the BPW91/6–31G* level. So far, only semi-empirical calculations and an NCA of a β-carotene model system have been reported. The mean deviations of the calculated bond distances and angles from β-carotene x-ray data are <1%. Because of the strict C_i symmetry constraints employed, all 282 normal modes of both configuration isomers were classified as either IR-active (a_u) or Raman-active (a_g). Owing to the validity of the mutual exclusion principle, which was shown exemplarily for the most intense bands in the FT-IR and the NIR-FT-Raman spectra, vibrational spectroscopic evidence for the centrosymmetry of β-carotene was obtained, to the best of our knowledge, for the first time. The different intensity ratios in the calculated Raman spectra of the two isomers could be explained by the corresponding eigenvectors and the resulting changes in polarizability, respectively. To the best of our knowledge, the eigenvectors of dominant normal modes of β-carotene are presented for the first time. Furthermore, the DFT calculations indicate that the s-*cis* isomer is 8.8 kJ mol^{-1} more stable than the all-*trans* form at the level of theory employed. Crystal packaging effects could be excluded because the quantum chemical calculations refer to the gas phase. Model systems for the polyene chain and the β-ionone rings were examined in order to separate relevant electronic contributions such as the conjugation of the terminal bonds from relevant steric contributions such as ring torsions. In contrast to β-carotene, the all-*trans* model system is 27.2 kJ mol^{-1} more stable than the s-*cis* model system. The absolute energies obtained from single point calculations on β-ionone rings showed that the ring torsions are reduced by 10.0 kJ mol^{-1} per ring for the ring conformation present in s-*cis*-β-carotene compared with that in the all-*trans* isomer. From these results it is concluded that the reduced conjugation length in s-*cis*-β-carotene, yielding an unfavorable electronic situation, is compensated by reduced ring torsions in comparison with all-*trans*-β-carotene.

In summary, the electronic structure calculations and the vibrational spectroscopic techniques employed reveal the centrosymmetric structure of an important natural product. Furthermore, the calculations on β-carotene and appropriate model systems, allowing a selective separation of electronic and steric contributions, reveal the origin of the higher stability of the natural abundant s-*cis*-β-carotene in comparison with its all-*trans* form.

Acknowledgments

Financial support from the German Science Foundation (Deutsche Forschungsgemeinschaft, Graduiertenkolleg 'Elektronendichte: Theory und Experiment'; GRK 690/1) and the Fonds der Chemischen Industrie is gratefully acknowledged.

REFERENCES

1. Mann J, Davidson RS, Hobbs JB, Banthorpe DV, Harborne JB. *Natural Products*. Addison Wesley Longman: Harlow, 1994.
2. Lehninger AL. *Principles of Biochemistry*. Worth: New York, 1982.
3. Saito S, Tasumi M.*J. Raman Spectrosc.* 1983; **14**: 310.
4. Hoskins LC. *J. Chem. Educ.* 1984; **61**: 460.
5. Mukai Y, Koyama Y, Ito M, Tsukida K. *J. Raman Spectrosc.* 1986; **17**: 387.
6. Koyama Y, Takatsuka I, Nakata M, Tasumi M. *J. Raman Spectrosc.* 1988; **19**: 37.
7. Merlin JC. *Pure Appl. Chem.* 1985; **57**: 785.
8. Robert B. *Adv. Photosynth.* 1996; **3**: 161.
9. Koyama Y, Fujii R. *Adv. Photosynth.* 1999; **8**: 161.
10. Robert B. *Adv. Photosynth.* 1999; **8**: 189.
11. Weesie RJ, Merlin JC, Lugtenburg J, Briton G, Jansen FJHM, Cornard JP. *Biospectroscopy* 1999; **5**: 19.
12. Hamaguchi H, Tasumi M. *Appl. Spectrosc.* 1986; **40**: 137.
13. Parker SF, Tavender SM, Dixon NM, Herman H, Williams K, Maddams WF.*Appl. Spectrosc.* 1999; **53**: 86.
14. Koch W, Holthausen MC. *A Chemist's Guide to Density Functional Theory*. Wiley-VCH: Weinheim, 2000.
15. Terstegen F, Buss V. *J. Mol. Struct. (Theochem*) 1998; **430**: 209.
16. Jensen F. *Introduction to Computational Chemistry*. Wiley: Chichester, 1999.
17. Garavelli M, Vreven T, Celani P, Bernardi F, Robb MA, Olivucci M. *J. Am. Chem. Soc.* 1998; **120**: 1285.
18. Garavelli M, Negri F, Olivucci M. *J. Am. Chem. Soc.* 1999; **121**: 1023.
19. González-Luque R, Garavelli M, Bernardi F, Merchán M, Robb MA, Olivucci M. *Proc. Natl. Acad. Sci. USA* 2000; **97**: 9379.
20. Bernardi F, Garavelli M, Olivucci M, Robb MA. *Mol. Phys.* 1997; **92**: 359.
21. Garavelli M, Bernardi F, Olivucci M, Robb MA. *J. Am. Chem. Soc.* 1998; **120**: 10210.
22. Zhi H, Sundström V, Pullerits T. *FEBS Lett*. 2001; **496**: 36.
23. Siebert T, Schmitt M, Engel V, Materny A, Kiefer W. *J. Am. Chem. Soc.* 2002; **124**: 6242.
24. Frisch MJ, Trucks GW, Schlegel HB, Scuseria GE, Robb MA, Cheeseman JR, Zakrzewski VG, Montgomery JA, Stratmann RE, Burant JC, Dapprich S, Millam JM, Daniels AD, Kudin KN, Strain MC, Farkas O, Tomasi J, Barone V, Cossi M, Cammi R, Mennucci B, Pomelli C, Adamo C, Clifford S, Ochterski J, Petersson GA, Ayala PY, Cui Q, Morokuma K, Malick DK, Rabuck AD, Raghavachari K, Foresman JB, Cioslowski J, Ortiz JV, Baboul AG, Stefanov BB, Liu G, Liashenko A, Piskorz P, Komaromi I, Gomperts R, Martin RL, Fox DJ, Keith T, Al-Laham MA, Peng CY, Nanayakkara A, Gonzalez C, Challacombe M, Gill PMW, Johnson B, Chen W, Wong MW, Andres JL, Gonzalez C, Head-Gordon M, Replogle ES, Pople JA. *Gaussian* 98, Revision A.7. Gaussian: Pittsburgh, PA, 1998.
25. Schaftenaar G, Noordik JH. *J. Comput. Aid. Mol. Des.* 2000; **14**: 123.
26. Senge MO, Hope H, Smith KM. *Z. Naturforsch. Teil C* 1992; **47**: 474.
27. Scott AP, Radom L. *J. Phys. Chem.* 1996; **100**: 16502.
28. Rauhut G, Pulay P. *J. Phys. Chem.* 1995; **99**: 3093.
29. Rush TS III, Kozlowski PM, Piffat CA, Kumble R, Zgierski MZ, Spiro TG. *J. Phys. Chem. B* 2000; **104**: 5020.
30. Stoll LK, Zgierski MZ, Kozlowski PM. *J. Phys. Chem. A* 2002; **106**: 170.